Materials Science Forum
ISSN: 1662-9752, Vol. 1182, pp 73-82
doi:10.4028/p-C1cyX0

Submitted: 2026-01-25
Revised: 2026-02-15
Accepted: 2026-02-20
Online: 2026-04-10

Application of a Discrete Finite Element Modeling Approach to Form a Near-Uniform Thickness Compound Curvature Composite Part

Kari D. White[1,a*] and James A. Sherwood[1,b]

[1]Department of Mechanical Engineering, University of Massachusetts, Lowell, One University Ave., 01854, Lowell, MA, USA.

[a]Kari_White@uml.edu; [b]James_Sherwood@uml.edu

Keywords: Composites, Finite Element, Thermoplastic, Thermoforming, Consolidation.

Abstract. Thermoforming of thermoplastic fiber-reinforced composites enables cost-effective production of complex, high-volume components, yet wrinkling and shear-induced thickness variations remain persistent challenges in compound-curvature geometries, often leading to nonuniform consolidation. This work presents a predictive virtual process simulation that integrates discrete mesoscopic finite element modeling with targeted blank design strategies to address these limitations. The approach, developed by the Sherwood Group and implemented in LS-DYNA, is applied to the thermoforming of a UHMWPE unidirectional cross-ply composite system (DSM® Dyneema® HB210). A thickness-stretch shell formulation (SHELL ELFORM25), coupled with a user-defined material model, is employed to simultaneously capture in-plane shear, through-thickness deformation, and frictional interactions during forming. A parametric study is conducted to evaluate the combined effects of tooling geometry and strategically introduced slits in the blank, including side- and corner-oriented configurations. The results demonstrate that the proposed formulation provides an effective balance between computational efficiency and predictive accuracy while explicitly reducing shear-induced thickening. Notably, corner-oriented slits at 45° to the fiber directions significantly reduced thickness variability and wrinkle severity compared to unmodified blanks and side-slit configurations. These findings highlight the novelty of integrating thickness-aware forming simulations with geometric blank modification as a robust pathway for achieving near-uniform thickness and improved preform quality in thermoformed composite parts.

Introduction

Wrinkling is a persistent defect when forming textile-reinforced composite blanks into double-curvature geometries, because the continuous sheet must accommodate incompatible in-plane strain states as it conforms to a hemispherical or helmet-like surface. Much of the composites forming literature has addressed wrinkle mitigation through process-level strategies, such as adjustments to forming pressure, tooling temperature, blank-holder conditions, or laminate architecture, while retaining continuous, uncut blanks. Although these approaches can delay the onset of wrinkling or reduce wrinkle severity, they do not fundamentally resolve the geometric incompatibility between a planar blank and a compound-curvature surface, and residual wrinkling in flange regions or along principal fiber directions is frequently observed. A review of military composite helmet manufacturing similarly identified wrinkling and fiber distortion as enduring challenges when forming highly curved structures from textile-based composites using continuous blanks [1]. From a mechanics perspective, numerical studies have further shown that wrinkling arises from global kinematic constraints governed by the interaction of tensile, in-plane shear, and bending stiffness, rather than purely local material response [2].

Intra-ply shear is the dominant mode of deformation during the forming process, and various degrees of material shearing are what allow the material to conform across a compound curvature part. Adding complexity to the forming process outcome is the increase in thickness of the lamina due to conservation of volume during in-plane shear. Dangora et al. [3] documented the incompressibility phenomenon with micrographs taken of laminates of DSM Dyneema® HB80

sheared to 0°, 20°, and 60° showing the associated thickness increases corresponding to conservation of volume. Based on that research, the resulting thickness in an area of the formed part can be correlated to the degree of shear in that area. The implications of thickness changes during the process are two-fold: (1) thickness variations in the preforms and (2) effects on tool/material friction during the forming.

Consider a two-step forming process. In Step 1, stacks of multiple plies are preformed one at a time. In Step 2, heat and pressure are applied in combination with matched dies to consolidate a stack of preforms and to cure the part. Figure 1 depicts how thickness variations in individual preforms can lead to poor-quality consolidation and voids due to pressure variations. Therefore, these thickness changes must be considered in a forming simulation. Ideally, a "uniform" thickness preform would resolve these manufacturing-induced defects associated with the consolidation step.

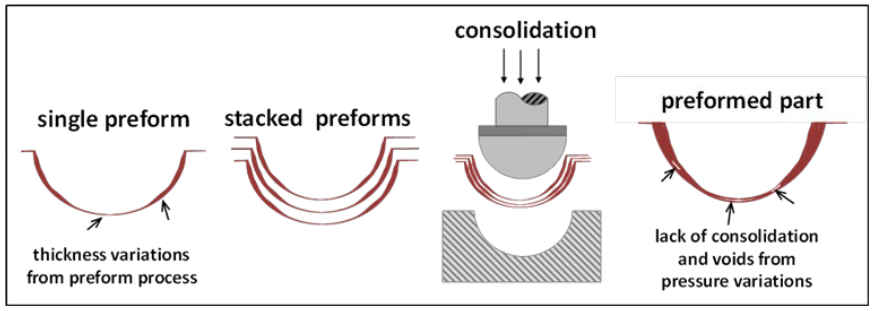

Fig.1. Variations in preform thickness lead to inconsistent/poor consolidation [14].

During the preforming step, the friction between the binder ring and the blank introduces in-plane tensile stresses that mitigate the wrinkling associated with shear deformation, but do not eliminate the change in thickness associated with shear. The resulting shear-induced thickness variations influence which areas of the material remain in contact with the binder ring during forming. Prior studies have shown that friction at sliding interfaces can lead to undesirable effects, including distortion of the final part geometry, residual stresses, and the formation of wrinkles [4-8]. Conversely, when binder rings are employed, controlled friction combined with appropriate binder-ring pressure can be used beneficially to restrain material flow and suppress wrinkle formation [3, 9-13]. In particular, hemispherical preforming trials conducted by Dangora et al. [3] demonstrated the strong dependence of wrinkle size and morphology on binder-ring pressure during the forming of a unidirectional cross-ply thermoplastic laminate (DSM Dyneema® HB80).

In a previous study by the authors [14], simulations of the experimental performing setup were completed to validate the material properties and friction values used in the simulations. Measured punch force, shear angle distribution, draw-in profile, and visual wrinkle distribution were metrics used in the evaluation. All simulations showed good correlation with the experimental results, and it was concluded that the modeling approach was valid to proceed with a parametric study of the tooling. The simulations were then used to find processing and tooling configurations that worked well in mitigating wrinkles and providing "uniform" thickness [15]. In that study, it was shown that tooling and blank shape also contribute to the uniformity of preform thickness, the development of wrinkles, and the overall quality of the preformed part. The gap between the binder ring and the punch, the gap between the die and the punch, and the radii of both the binder ring and the die are parameters that can be altered to influence the preform results. All simulations used flat blanks without slits or darts.

Classical textile mechanics establishes that darts and gores are a geometric necessity for draping flat woven fabrics over spherical surfaces without wrinkling [16]. Past works by others have demonstrated that blank segmentation, through the introduction of strategic slits, relief cuts, or dart-like features, can address the geometric constraints that lead to wrinkling by locally releasing in-plane compressive stresses. In the context of thermo-hydroforming of composite helmets, Ahn et al. [17] explicitly treated the blank shape and the relief cuts made in the blank as design variables in a numerical optimization framework aimed at minimizing wrinkle density and wrinkle height, showing that appropriately designed V-shaped relief cuts significantly reduced wrinkling and improved

thickness uniformity. Related studies by Ahn et al. [18] further emphasized the importance of integrating considerations of forming kinematics, material architecture, and blank design in helmet-like thermo-hydroformed components. Experimental work by Hu et al. [19] on hemispherical forming of continuous fiber-reinforced textile preforms demonstrated that precision slitting in high-shear regions reconfigured deformation paths, delayed the onset of shear locking, and suppressed global wrinkling. Similar geometric modification strategies were also reported by Kim et al. [20] in double-diaphragm forming, where pre-cut prepregs were employed to improve part quality in complex geometries.

In contrast to prior works that optimize relief-cut geometry primarily through numerical or process-level studies, the present work implements and evaluates slit/dart strategies directly within the thermoforming of fiber-reinforced composite blanks of DSM® Dyneema® HB210, with the dual objectives of mitigating wrinkling and reducing thickness variations across the surface of the formed part. One of the promising configurations from the previous research [15] was used as a baseline for modifying the blank in the current research. The results of this investigation lay the foundation for using the proposed methodology to design tooling and incorporate strategic cuts in the blank to mitigate wrinkling and reduce thickness variations during the forming of compound curvature parts.

Methodology

Modeling Approach. The Sherwood Group [21] developed a discrete modeling approach that has been shown to simulate the forming of a plain-weave hemisphere shape with good accuracy. Conventional elements available in commercial finite element software are used in the unit cell approach shown in Figure 2. Fiber directionality is described and tracked by beam elements that represent the tensile and flexural properties of the laminate. In the current research, which uses LS-DYNA, the shear load is carried by thickness-enhanced shell elements (thick-thin shell), SHELL ELFORM25, that capture the evolution of the in-plane shear stiffness as a function of the degree of shear, as well as linear strain through the thickness. The initial thickness is prescribed in the section definition keyword card set. In the case of woven materials, the horizontal and vertical beams represent the warp and weft tows with a bilinear modulus for the beam elements to capture wrinkling behavior [22]. In the case of the 0/90 cross-ply considered in the current research, the horizontal and vertical beams can be assigned tensile and flexural properties of the 0° and 90° layers.

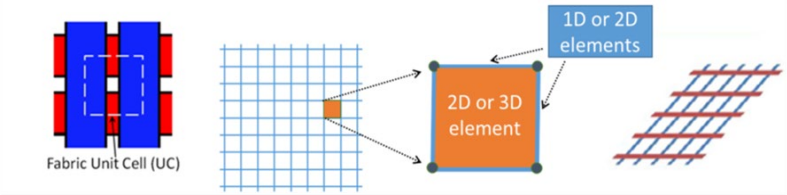

Fig. 2. Unit cell configuration for mesoscopic laminate material model [14].

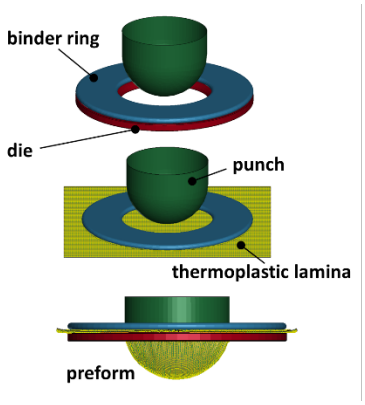

Fig. 3. Hemisphere preform simulation in LS-DYNA [15].

The hemisphere preform model as shown in Figure 3 was built to replicate the experimental setup; the tooling geometry was then modified to represent the binder ring and die sizes. The friction coefficients for the material were calculated from data recorded using the UMass Lowell friction tester, as redesigned by Campshure et al. [14, 23, 24].

The composite laminate system investigated in this research is DSM® Dyneema® HB210. This material system is a thermoplastic cross-ply containing four unidirectional layers oriented in a $(0/90)_2$ fiber configuration with each ply comprised of UHMWPE fibers and a thermoplastic polyurethane (TPU) based matrix [25]. The tensile, shear and bending properties at 100°C for Dyneema® HB210 are provided from previous testing [5, 26, 27] and shown in Table 1, where γ is defined as the shear strain of the composite lamina. The friction values are averages of fiber orientation and resin condition, as the hemisphere is symmetrical and each condition is represented equally.

Table 1. Material Properties for Hemisphere Preforming Simulations (MPa)

Shear Stiffness as a Function of Shear Strain (MPa)	Tensile Modulus (MPa)	Compressive Modulus (MPa)	Tool/Ply Static Friction	Tool/Ply Dynamic Friction
$1723\|\gamma\|^6-5002\|\gamma\|^5+5677\|\gamma\|^4-3179\|\gamma\|^3+909\|\gamma\|^2-125\|\gamma\|+7$	19300	5000	0.110	0.077

Parametric Study. Tooling Geometry Parameters. Specific geometry attributes were identified to be relevant to the preforming outcomes. Figure 4 shows the upper gap as the distance between the inner radius of the binder ring and the outer radius of the punch. The lower gap indicated the distance between the inner radius of the die and the punch. The lower radius is a measure of the fillet, or curvature, of the die.

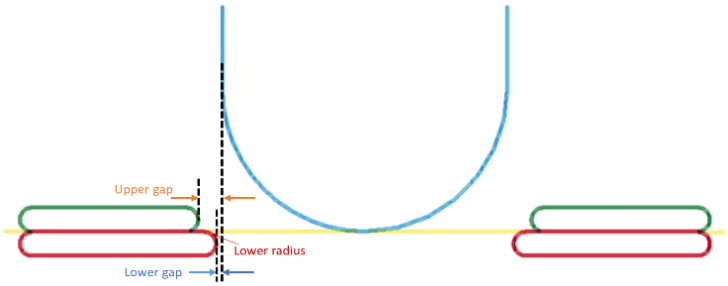

Fig. 4. Tooling parameters analyzed in study [15].

The experimental preform setups had the geometric values listed in Table 2, and the simulations were created to reflect these values. An initial parametric study was conducted that used combinations of the existing tooling to evaluate the sensitivity of the model to parameter changes. A binder pressure of 300 kPa was used to replicate the experimental pressure used with the four layers of laminate with the redesigned tooling. All simulations were performed with the properties of DSM® Dyneema® HB210 at a processing temperature of 100°C. One set of tooling that showed promising results for wrinkle mitigation, in terms of wrinkle distribution and average wrinkle height, and uniform material thickness in the hemispherical area had tooling dimensions listed in Table 2.

The preform quality and thickness profile are shown in Figure 5.

Figure 5(a) is a uniform color to allow a clear view of the wrinkle distribution in the part and their heights.

Figure 5(b) shows the final thickness distribution in the part. The thickest areas are in the ±45° regions.

Table 2. Geometric Properties of Baseline Tooling

Upper Gap [mm]	Lower Gap [mm]	Lower Radius [mm]
12.7	3.18	10.2

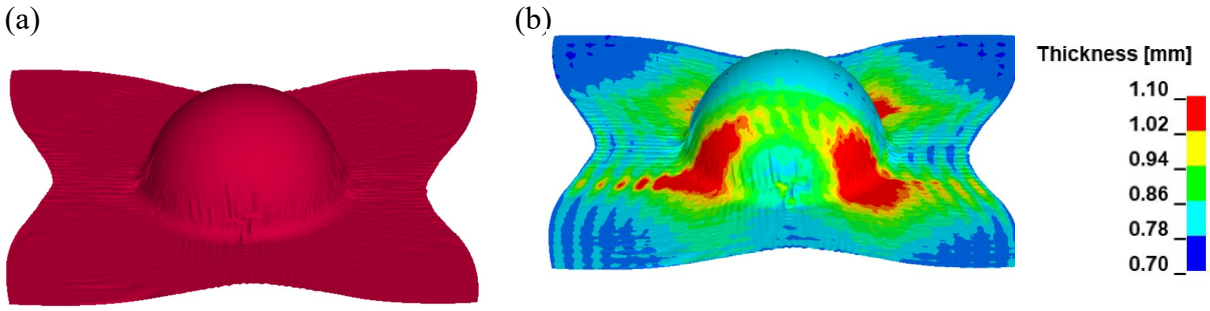

Fig. 5. Baseline tooling configuration used for blank slit study:
(a) Formed part showing distribution of wrinkles (b) Thickness variation denoted by color contours

Blank Slit Study. One method of reducing wrinkles is to remove part of the blank material, allowing the fibers to move freely in local areas. The next set of investigations was planned to determine whether adding relief areas, via slits in the material, would not only aid wrinkle mitigation but also reduce thickness variations. Two types of slits were introduced to the square blank material: slits that extended horizontally and vertically from the midsides of the square blank and slits that extended at 45° into the blank from the corners of the square. Eight slit sizes were investigated for each type of slit. For each slit size, the square "Area between slits", as denoted in Figure 6, was kept the same to be able to compare side and corner slits. The dimensions and mean values for each of the slit configurations that were investigated are provided in Table 3.

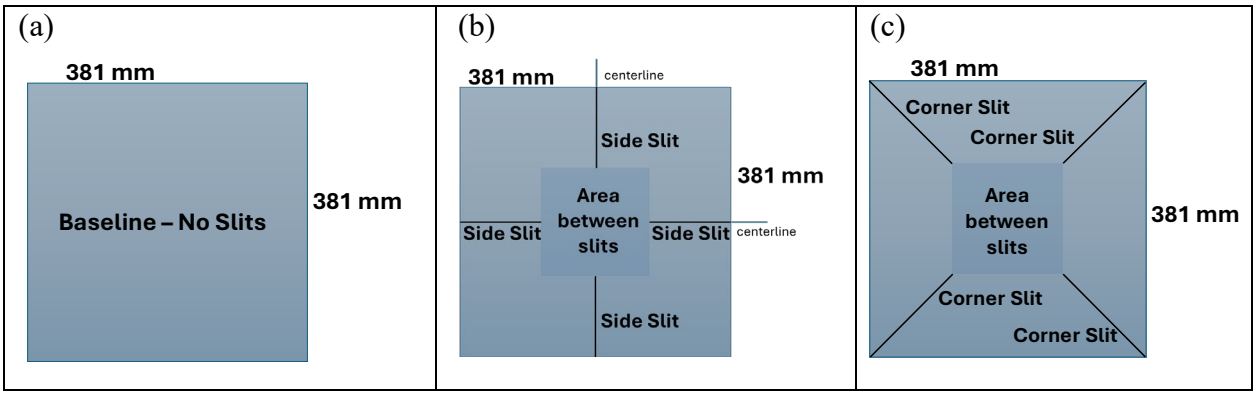

Fig.6. Blank configurations: (a) Baseline [no slits], (b) Blank with slits from sides of square blank, and (c) Blank with slits from corners of square blank.

Three metrics were used in comparing the results from the study, i.e., (1) Thickness distribution, (2) Wrinkle Height, and (3) In-plane shear angle distribution. The thickness distribution over the hemispherical portion of the preform gives guidance on how well the preform can be consolidated into a uniform part. As controlling thickness uniformity is a goal of this project, measures of thickness variation were used as a quantitative comparison. Wrinkle heights were quantified by outputting the location of every shell node within the hemispherical portion of the preform, then determining the distance of each node from the surface of the punch. Finally, the in-plane shear angle distribution contributes to both the thickness uniformity, and an indication of how well the binder ring can engage appropriate shearing of the laminate into the hemispherical shape.

Results and Discussion

The initial thickness of one ply of the DSM® Dyneema® HB210 material was 0.72 mm, and the final thicknesses of the elements over the hemisphere portion of the preform were normalized to this initial thickness to evaluate the relative change in thickness. Box-and-whisker plots were used to visualize the distribution of element thickness across the part. Figure 7 shows normalized thickness results for all 16 slit configurations that were analyzed, as well as the baseline square blank. The box for each

configuration represents the middle 50% of the data, while the lines extending to the top and bottom represent the max and min data values.

In addition to thickness uniformity, wrinkle height provides a complementary measure of out-of-plane defect severity and is presented here immediately following the thickness results for direct comparison. Wrinkle height is a critical quality metric, as fewer, smaller wrinkles than in the baseline configuration are desirable. However, quantifying wrinkles is more complex than discerning the thickness variations. Figure 8 shows the wrinkle heights for all configurations, with the X marking the mean height. Note that the wrinkle height was defined as the distance of the node from the punch, which means that if the material is in contact with the punch, then the wrinkle height would be half the thickness of the material at that point. Mean wrinkle height is used here as a scalar metric to evaluate the average size of wrinkles over the part. Alternative geometry-based wrinkle metrics have been reported in the literature, such as the wrinkle index introduced by Chen et al. [28], which quantifies wrinkle severity using local surface normal variation extracted from finite element simulations. While conceptually different from the wrinkle-height definition adopted in the current research, both approaches aim to capture out-of-plane deformation associated with forming-induced defects.

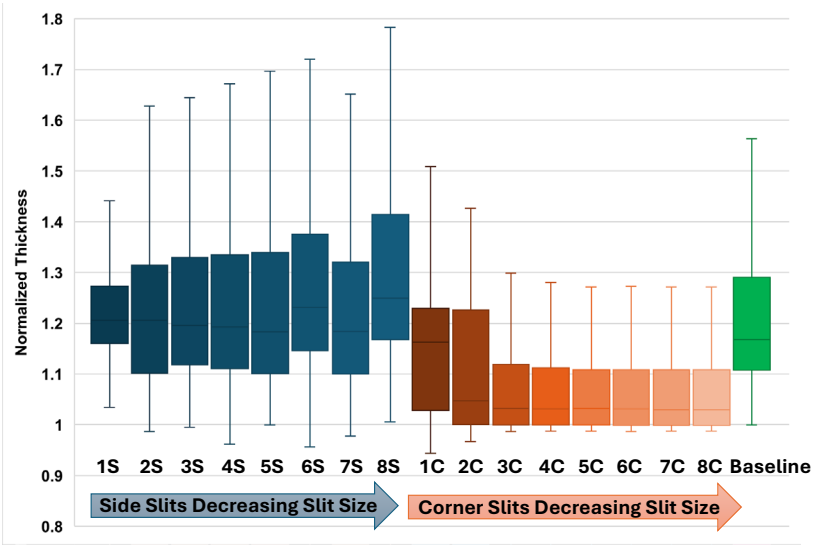

Fig. 7. Normalized thickness variation for all slit configurations.

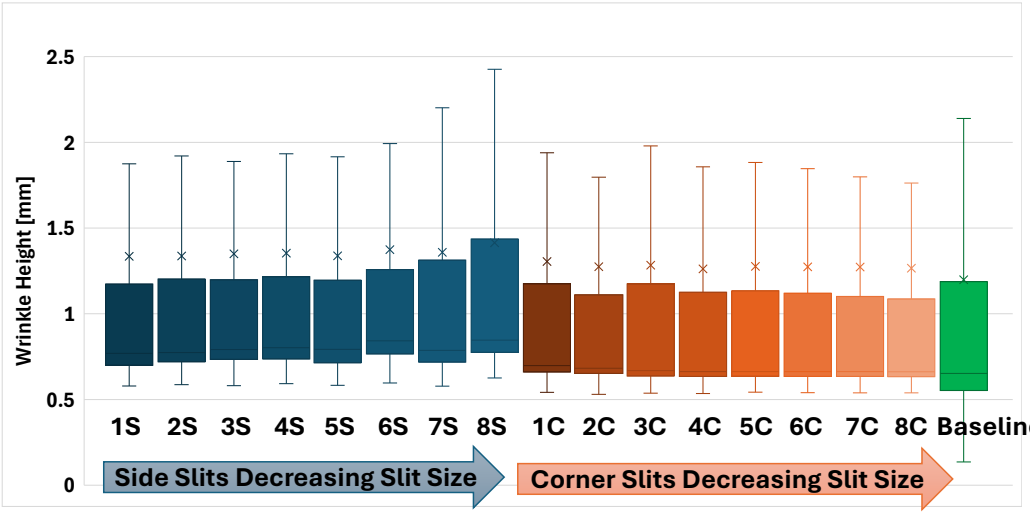

Fig. 8. Wrinkle height for all slit configurations.

The goal is to minimize thickness variation. Therefore, the tighter (or narrower) the box and the smaller the whiskers, i.e., the range between the maximum and minimum, the better in Figure 8. The mean normalized thickness of the baseline blank was 1.22 (SD = 0.16), indicating moderate variation.

Again, this tooling geometry was selected based on the quality of the preform. Adding side slits reduced variation in two configurations (1S and 2S) relative to the baseline, as indicated by a decrease in standard deviation; however, these configurations have the least material in the center of the blank without slits, so the slits will extend into the hemispherical portion of the preform. The other side slit configurations did not improve the thickness uniformity. Discontinuities in the material are undesirable in most applications due to a loss of strength. The corner slits performed remarkably well at maintaining uniform thickness, even with small slits applied to the blank material. The average normalized thickness of configuration 8C, which has the largest intact central material, is 1.07, with a standard deviation of 0.10, an improvement over the baseline configuration. Figure 9 shows the thickness distribution across the part for configurations 1S, 8C, and the baseline. The slight asymmetry observed in the thickness distribution in Figure 9a is attributed to a numerical effect associated with the use of an explicit time-integration solver rather than a physical asymmetry in the model.

Table 3. Sample Dimensions and Mean Values

Sample Name	Side Length of Center Area (mm)	Slit Length (mm)	Mean Normalized Thickness	Standard Deviation Normalized Thickness	Mean Wrinkle Height (mm)	Standard Deviation Wrinkle Height (mm)
1S	25	178	1.23	0.10	1.34	1.26
2S	51	165	1.21	0.12	1.34	1.24
3S	76	152	1.24	0.16	1.35	1.23
4S	102	140	1.24	0.17	1.35	1.21
5S	127	127	1.25	0.20	1.34	1.21
6S	152	114	1.29	0.21	1.37	1.18
7S	178	102	1.23	0.18	1.36	1.23
8S	203	89	1.31	0.20	1.41	1.18
1C	25	257	1.14	0.10	1.31	1.29
2C	51	244	1.11	0.12	1.27	1.28
3C	76	231	1.08	0.12	1.28	1.29
4C	102	219	1.07	0.10	1.26	1.27
5C	127	206	1.07	0.10	1.28	1.31
6C	152	193	1.07	0.10	1.27	1.30
7C	178	181	1.07	0.10	1.27	1.30
8C	203	168	1.07	0.10	1.27	1.30
Baseline	381	NA	1.22	0.16	1.20	1.26

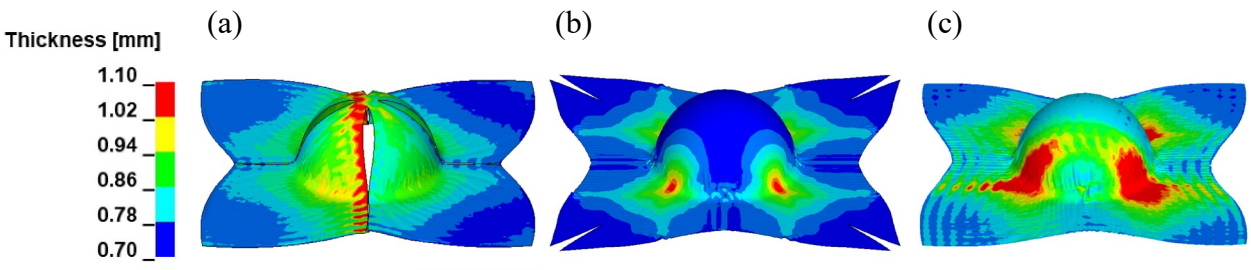

Fig. 9. Thickness variations over the hemisphere portion of the preform for configurations (a) 1S, (b) 8C, and (c) baseline configurations.

The baseline configuration has a mean wrinkle height of 1.20 mm, while the best side-slit configuration has a mean height of 1.34 mm (1S), and the corner-slit configuration has a mean height of 1.26 mm (4C). As in the thickness study, the best side-slit configuration is also one with very long slits that would extend into the material. Although the corner-slit configuration with the smallest average is not the one with the smallest slits, the improvements in slit size from 8C are minimal.

Future work on wrinkle height should include subtracting the material thickness at the location, or employ another method of normalizing the data for comparison.

Summary

In this research, hemisphere preforming simulations were performed on a unidirectional thermoplastic cross-ply material system, DSM Dyneema® HB210. A parametric study was performed to evaluate the role of the binder gap (space between the punch and the binder) and the die radius (the curvature of the die that the material is pushed through). Results showed corner slits outperform side slits in wrinkle control and thickness uniformity, with smaller slits outperforming larger ones. Side slits show increasing wrinkle height and thickness variability with smaller slits, indicating potential process challenges. Future studies will normalize the wrinkle distribution for better quantification.

Acknowledgements

This work was performed under Cooperative Agreement W911NF-18-2-0033 with the US Army Research Lab. The material was donated by DSM, and LS-DYNA was donated by ANSYS.

References

[1] Liang Y, Chen X, Soutis C. Review on manufacture of military composite helmet. Applied Composite Materials. 2022;29(1):305-23. https://doi.org/10.1007/s10443-021-09944-3

[2] Boisse P, Hamila N, Vidal-Sallé E, Dumont F. Simulation of wrinkling during textile composite reinforcement forming. Influence of tensile, in-plane shear and bending stiffnesses. Composites Science and Technology. 2011; 71(5): 683-92. https://doi.org/10.1016/j.compscitech. 2011.01.011

[3] Dangora LM, Mitchell CJ, Sherwood J, Parker JC. Deep-Drawing Forming Trials on a Cross-Ply Thermoplastic Lamina for Helmet Preform Manufacture. Journal of Manufacturing Science and Engineering. 2017;139(3):031009.

[4] Ersoy N, Potter K, Wisnom MR, Clegg MJ. An experimental method to study the frictional processes during composites manufacturing. Composites Part A: Applied science and manufacturing. 2005;36(11):1536-44.

[5] Ersoy N, Garstka T, Potter K, Wisnom MR, Porter D, Stringer G. Modelling of the spring-in phenomenon in curved parts made of a thermosetting composite. Composites Part A: Applied Science and Manufacturing. 2010;41(3):410-8.

[6] Larberg YR, Åkermo M. On the interply friction of different generations of carbon/epoxy prepreg systems. Composites Part A: Applied Science and Manufacturing. 2011;42(9):1067-74.

[7] Lightfoot JS, Wisnom MR, Potter K. A new mechanism for the formation of ply wrinkles due to shear between plies. Composites Part A: Applied Science and Manufacturing. 2013; 49: 139-47.

[8] Arafath ARA, Vaziri R, Poursartip A. Closed-form solution for process-induced stresses and deformation of a composite part cured on a solid tool: part I–flat geometries. Composites Part A: Applied Science and Manufacturing. 2008;39(7):1106-17.

[9] Breuer U, Neitzel M, Ketzer V, Reinicke R. Deep drawing of fabric-reinforced thermoplastics: Wrinkle formation and their reduction. Polymer composites. 1996;17(4):643-7.

[10] Lee JS, Hong SJ, Yu W-R, Kang TJ. The effect of blank holder force on the stamp forming behavior of non-crimp fabric with a chain stitch. Composites science and technology. 2007;67(3-4):357-66.

[11] Lin H, Wang J, Long A, Clifford M, Harrison P. Predictive modelling for optimization of textile composite forming. Composites Science and Technology. 2007;67(15-16):3242-52.

[12] Obermeyer E, Majlessi SA. A review of recent advances in the application of blank-holder force towards improving the forming limits of sheet metal parts. Journal of Materials Processing Technology. 1998;75(1-3):222-34.

[13] Akkerman R, Ten Thije R, Sachs U, De Rooij M, editors. Friction in textile thermoplastic composites forming. Proceedings of the 10th international conference on textile composites-TEXCOMP; 2010.

[14] White KD, Campshure B, Sherwood JA. Effects of Thickness Changes and Friction during the Thermoforming of Composite Sheets. ESAFORM 2021 24th International Conference on Material Forming; Liège, Belgique2021.

[15] White KD, Sherwood JA. An investigation into the relationship between hemisphere tooling parameters and thickness changes during the thermoforming of a thermoplastic composite. Materials Research Proceedings. 2024;41:513-22. https://doi.org/10.21741/9781644903131-57

[16] Hu J. Structure and mechanics of woven fabrics: CRC press; 2004.

[17] Ahn H, Kuuttila NE, Pourboghrat F. Effects of pressure, boundary conditions, and cutting reliefs on thermo-hydroforming of fiber-reinforced thermoplastic composite helmet based on numerical optimization. Journal of Thermoplastic Composite Materials. 2021;34(2):181-202. https://doi.org/10.1177/0892705719842631

[18] Ahn H, Kuuttila NE, Pourboghrat F. Thermo-hydroforming of a fiber-reinforced thermoplastic composites considering fiber orientations. AIP Conference Proceedings. 2018;1960(1):020002. https://doi.org/10.1063/1.5034803

[19] Hu J, Legrand X, Wang P. Optimizing continuous fiber-reinforced textile preforms forming: Minimizing wrinkling through precision slitting. Thin-Walled Structures. 2025;210:113052. https://doi.org/10.1016/j.tws.2025.113052

[20] Kim S, Shin H, Lee K, Ha S. Enhancing Product Performance via a Modified Double-Diaphragm Forming (mDDF) Preform Method for Prepreg Compression Molding of Fiber-Reinforced Polymer Composites. Polymers. 2025;17(11):1489. https://doi.org/10.3390/polym17111489

[21] Jauffres D, Sherwood J, Morris C, Chen J. Discrete mesoscopic modeling for the simulation of woven-fabric reinforcement forming2010. 1205-16 p.

[22] Dangora LM, Mitchell CJ, Sherwood JA. Predictive model for the detection of out-of-plane defects formed during textile-composite manufacture. Composites Part A: Applied Science and Manufacturing. 2015;78:102-12.

[23] Fetfatsidis KA, Gamache LM, Gorczyca JL, Sherwood JA, Jauffrès D, Chen J. Design of an apparatus for measuring tool/fabric and fabric/fabric friction of woven-fabric composites during the thermostamping process. International Journal of Material Forming. 2013;6(1):1-11. https://doi.org/10.1007/s12289-011-1058-3

[24] Campshure B, White KD, Sherwood JA. Friction Characterization of UHMWPE Cross-Ply Composite Sheets for Thermoforming Processes. ESAFORM 2021 24th International Conference on Material Forming; Liège, Belgique2021. https://doi.org/10.25518/esaform21.759

[25] DSM Dyneema (R) Industries 2018 [Available from: http://www.dsm.com/products/dyneema/en_US/home.html.

[26] White KD, Krogh C, Sherwood JA, editors. Investigation of shear characterization of a UHMWPE unidirectional cross-ply for finite element simulation of composite processing. AIP Conference Proceedings; 2019: AIP Publishing LLC.

[27] White K, Yeager M, Sherwood J, Bogetti T, Cline J. Material Characterization and Finite Element Modeling for the Forming of Highly Oriented UHMWPE Thin Film and Unidirectional Cross-ply Composites. ASC 33rd Technical Conference; Seattle, WA2018.

[28] Chen S, Thompson AJ, Dodwell TJ, Hallett SR, Belnoue JPH. Fast optimisation of the formability of dry fabric preforms: A Bayesian approach. Materials & Design. 2023;230:111986. https://doi.org/10.1016/j.matdes.2023.111986